

## New Research on MEMS Acoustic Vector Sensor Used in Ground Marker of Pipeline

Liu Meng-ran<sup>1,2</sup>, Zhang Guo-jun<sup>1,2</sup>, Jian Ze-ming<sup>\*1</sup>, Liu Hong<sup>1</sup>, Song Xiao-peng<sup>1</sup>,  
Zhang Wen-dong<sup>1,2</sup>

<sup>1</sup>Key Laboratory of Instrumentation Science & Dynamic Measurement, Ministry of Education,  
North University of China, Taiyuan 030051, China;

<sup>2</sup>Key Laboratory Of Science and Technology on Electronic Test & Measurement,  
North University of China, Taiyuan 030051, China

\*Corresponding author, e-mail: jianzemingx@163.com

### Abstract

Recently, ground marker based on the principle of acoustic detection has become the trend of pipeline technology. As to the difficulty and low accuracy of ground marker, this paper introduces a new MEMS bionic acoustic vector sensor with high sensitivity, good performance in low frequency and lower power. As to the problem of the port/starboard blur of this vector sensor in ground marking, it proposes a new plan and proves the correctness of the plan through theoretic analysis and experimental verification. The results show that the mean error of the directional angle is within 5 degree meeting the needs of the engineering project.

**Keywords:** pipeline ground marking, MEMS vector sensor, the port/starboard blur, direction angle

**Copyright © 2014 Institute of Advanced Engineering and Science. All rights reserved.**

### 1. Introduction

Pipeline transportation has become one of five top transportation mode to keep pace with aviation, railway, road and water transport and has played an increasingly larger role in the national economy and national defense construction [1]. Meanwhile, the accidents of pipeline leak happen frequently with the age of pipeline, the corrosion of pipeline and the artificial. Pipeline inspection gauge designed for pipeline defect detection is an important detection equipment. While pipeline inspection gauge works in the pipeline, it would generate about 1m error per 1km. The longer the pipeline is, the greater the cumulative error would be generated and the less accurate position would be got [2-4]. So, for long-distance pipeline defect detection, the inspection gauge must be marked once a kilometer in the process of moving. The time when the pipeline inspection gauge is getting through the marking point is ascertained by the ground marker of pipeline. Then by comparing to the count of the mileage wheel in the moment, the count value of the Mileage wheel was corrected to eliminate the accumulated error, and get the accurate positioning of the defect. In recent years, with the rapid development of the pipeline industry, domestic and foreign companies are actively looking for new principles and methods of tracking markers. The design of positioning system based on the principle of acoustic is simple, easy to achieve, suitable for real-time processing and with higher sensitivity and a wide range of the detection.

In this paper the MEMS bionic acoustic vector sensor with high sensitivity, good performance in low frequency and lower power has been used in ground marker. And when it was used to accurate the position of the pipeline inspection gauge, a new scheme eliminating the problem of the port/starboard blur has been put forward.

### 2. The Working Principles and Mathematical Model

#### 2.1. The Working Principles [5-7]

MEMS bionic acoustic vector sensor based on the piezoresistive principle can measure the low frequency till the Zero. High sensitivity, good performance in low frequency and low power make it a unique advantage in measuring the weak signals. MEMS vector sensor has been shown in Figure 1.



Figure 1. Objective graph of MEMS acoustic vector sensor

MEMS bionic acoustic vector sensor is based on silicon and composed of four-arm silicon microstructure with a standard piezoresistive silicon micromachining process and rigid cylindrical body fixed in the center of the beam. Structure model is shown in Figure 2. There are eight equal-value strain varistor, R1, R2, R3, R4, R5, R6, R7 and R8, made by means of diffusion in the four-arm. R1, R2, R3 and R4 constitute a Wheatstone bridge, and R5, R6, R7 and R8 constitute another. The distribution of piezoresistor on the micro-structure is shown in Figure 3 and composition of the Wheatstone bridge is shown in Figure 4.

When the vibration signal of X-direction acts on the micro-structure, the beam will produce asymmetrical stress distribution, if R1 and R3 correspond to the tension, R2 and R4 would correspond to the pressure and R5, R6, R7 and R8 would correspond to the shear force. When the width of the beam is much greater than the thickness, the shear deformation can be ignored. In this situation we can basically treat that R5, R6, R7 and R8 change nothing, while the resistance values of (R1, R3) and (R2, R4) change into the opposite direction; When the vibration signal of Y-direction acts on the micro-structure, the beam will produce asymmetrical stress distribution, if R5 and R7 correspond to the tension, R6 and R8 would correspond to the pressure and R1, R2, R3 and R4 would correspond to the shear force. When the width of the beam is much greater than the thickness, the shear deformation can be ignored. In this situation we can basically treat that R1, R2, R3 and R4 change nothing, while the resistance values of (R5, R6) and (R7, R8) change into the opposite direction.

When a signal is applied to the sensor, it can be decomposed into X-direction and Y-direction, cantilevers have been deformed and Wheatstone bridges have been changed. According to the outputs of the wheatstone bridge changing, we can determine the direction of signal source.

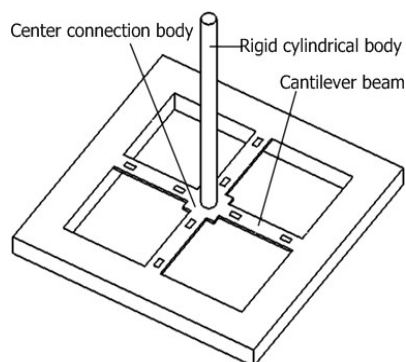


Figure 2. Diagram of the acoustic sensor microstructure model

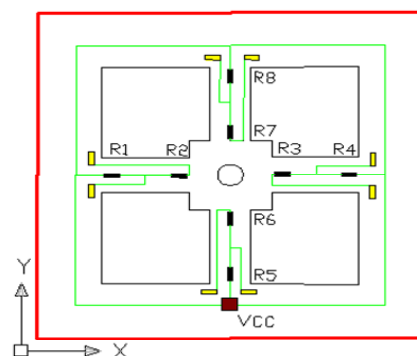


Figure 3. Diagram of connection of distribution of piezotransistor on the micro structure

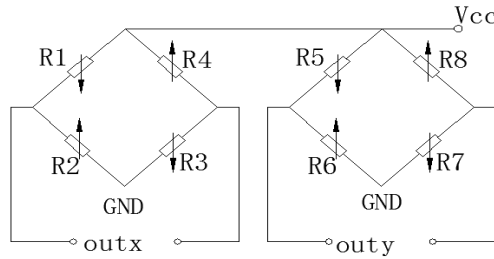


Figure 4. Photo of wheatstone bridge formed by piezatransistor

**2.2. Mathematical Model Analysis [8-10]**

When the cylinder of the sensor microstructure suffer the load force of X-direction, the force  $F_x$  will generate two components in the center block of the micro structure, the horizontal force  $F_H$  along the X-axis direction and torque  $M$  around the Y-axis. Since the mess of center block of microstructure is much smaller than the cylinder, so it can be ignored in the calculation.

The mechanical analysis model of the microstructure has been established and shown in Figure 5-7. Figure 5 shows the movement of accelerometer when subjected to a normal horizontal acceleration. Figure 6 shows the force analysis about central block, and Figure 7 shows the force analysis about single cantilever. If  $F_x$  direction is in the positive direction of the X-axis, the four resistors ( $R_1$ ,  $R_2$ ,  $R_3$  and  $R_4$ ) in the cantilever in turn show the pressure (-), tension (+), pressure (-) and tension (+), that is  $R_1$  decreases,  $R_2$  increases,  $R_3$  decreases and  $R_4$  increases. If  $F_x$  direction is in the negative direction of the X-axis, the four resistors ( $R_1$ ,  $R_2$ ,  $R_3$  and  $R_4$ ) in the cantilever in turn show the tension (+), pressure (-), tension (+) and pressure (-), that is  $R_1$  increases,  $R_2$  decreases,  $R_3$  increases and  $R_4$  decreases.

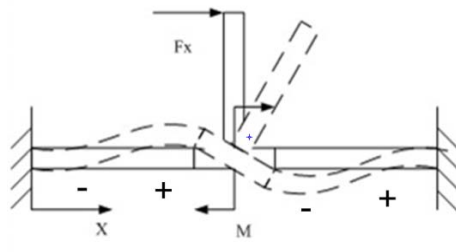


Figure 5. Movement of accelerometer when subjected to a normal horizontal acceleration

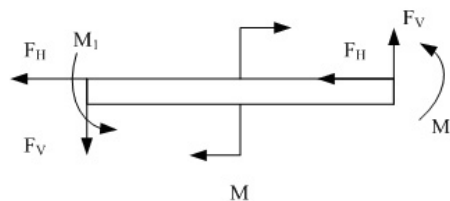


Figure 6. Photo of force analysis about center block of the micro structure



Figure 7. Photo of force analysis about single cantilever

By the mechanics of material theory:

The stress  $\sigma_{(x)}$  of any point in the single cantilever under the actions of bending moment  $M_{(x)}$  and horizontal force  $F_H$  can be expressed as:

$$\sigma_{(x)} = \pm \frac{L^2 + 3aL - 3x(a+L)}{\frac{2}{3}bt^2(L^2 + 3aL + 3a^2)} M \pm \frac{F_H}{bt} \quad (1)$$

In the formula:  $L(\mu\text{m})$  is the length of cantilever;  $b(\mu\text{m})$  is the width of the cantilever;  $t(\mu\text{m})$  is the thickness of the cantilever;  $a(\mu\text{m})$  is the half-width of the center block.

### 3. New Scheme of the Position Determination

In the case of no stress, resistance in the X-direction bridge does not change, and the bridge balances. When the stress exist, the resistance of the varistor would change. Output voltage in X-direction can be expressed as:

$$V_{outx} = \frac{(R_1 + \Delta R_1)(R_3 + \Delta R_3) - (R_2 - \Delta R_2)(R_4 - \Delta R_4)}{(R_1 + \Delta R_1 + R_2 - \Delta R_2)(R_3 + \Delta R_3 + R_4 - \Delta R_4)} V_{in} \quad (2)$$

Here,  $R_1 = R_2 = R_3 = R_4$ ,  $\Delta R_1 = \Delta R_2 = \Delta R_3 = \Delta R_4 = \Delta R$ . In the formula,  $V_{in}$  is the input voltage. Formula (2) can be approximately expressed as:

$$V_{outx} = \frac{\Delta R}{R} V_{in} \quad (3)$$

When a vibration signal (which can be seen as a sinusoidal signal) acts on the sensor, the output voltages in X-direction and Y-direction are  $V_x$  and  $V_y$ , respectively. Due to the direction of the pipeline buried has been known, what only need to do is to determine the orientation from zero to 180 degrees. Two Wheatstone bridges have actually measured the voltage difference between the resistors ( $R_2$  and  $R_3$ ) and ( $R_6$  and  $R_7$ ), respectively. And the final testing voltage has been output after the voltage difference going by the differential amplifier circuit. And if the voltage across the resistor  $R_2$  is greater than the voltage across  $R_3$ ,  $V_x$  is positive, otherwise  $V_x$  is negative; the voltage across the resistor  $R_6$  is greater than the voltage across  $R_7$ ,  $V_y$  is positive, on the other hand,  $V_y$  is negative.

We can get the direction angle of the Pipeline inspection gauge (sound source)  $\theta$  is  $\arctan(V_y / V_x)$  ( $0^\circ < \theta \leq 90^\circ$ ) by calculating. If the sound source in the first quadrant, the direction angle of the sound source  $\theta$  is  $\arctan(V_y / V_x)$ ; If the sound source in the second quadrant, the direction angle of the sound source is  $180^\circ - \theta$ . Determination of sound source is shown in Figure 8. By analyzing the trends and relationships of the output voltages of the  $V_x$  and  $V_y$ , determine the specific location of the sound source (in the first or second quadrant).

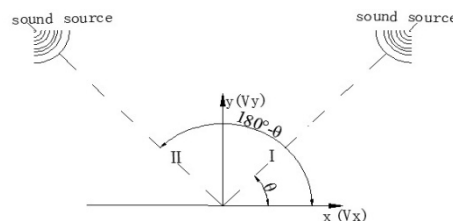


Figure 8. Diagram of determination of sound source

When the sound source is in the first quadrant,  $R_2$  and  $R_6$  are suffering the same normal stress or negative stress (changing synchronously).  $R_3$  and  $R_7$  also change

synchronously. But R2 and R3 (R6 and R7) change asynchronously. Output voltage of bridge  $V_{outx}$  in X-direction going by the differential mode amplifier circuit is  $V_x$ , and Output voltage of bridge  $V_{outy}$  in Y-direction going by the differential mode amplifier circuit is  $V_y$ .  $V_x$  and  $V_y$  are suffering the same normal stress or negative stress (changing synchronously); When the sound source is in the second quadrant, R2 and R6 are respectively suffering the normal stress and the negative stress (changing asynchronously). R3 and R7 change asynchronously. And R2 and R3 (R6 and R7) change asynchronously. Output voltage of bridge  $V_{outx}$  in X-direction going by the differential mode amplifier circuit is  $V_x$ , and Output voltage of bridge  $V_{outy}$  in Y-direction going by the differential mode amplifier circuit is  $V_y$ .  $V_x$  and  $V_y$  change asynchronously. According to the relationship between  $V_x$  and  $V_y$ , we can make sure the sound source (distinguishing I and II quadrant).

#### 4. Analysis and Verification of the Experimental Testing Result

In the experiment, the sensor is vertically downward, and sensing head buried in the soil tight and heavy (in Figure 9), ensuring that the sensor is coupled with soil well.

In order to simulate the friction acoustic signals of the pipeline inspection gauge running in the pipeline better, we can use the way of tapping on the ground to simulate it. By collecting and analyzing the tapping signals, we can find the tapping signals are in 80HZ-300HZ (in Figure 10) which are included in the spectral range of the friction signal of the pipeline inspection gauge running in the pipeline. To a certain extent, tapping signals could simulate the actual acoustic signal.



Figure 9. Method of the MEMS acoustic vector sensor buried

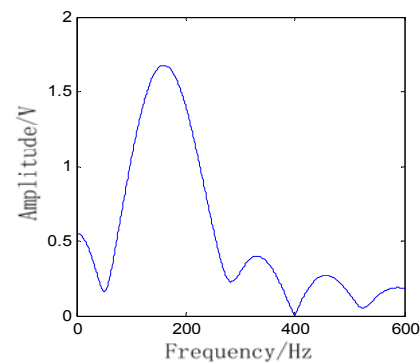


Figure 10. Spectrum of the beating signal

First of all, when MEMS vector acoustic sensor is placed, semicircle is painted with acoustic sensor as the center and  $r$  as the radius of the circle. On the semicircle, draw a point every  $10^\circ$  and draw the point of zero to 180 degrees. Sensor experimental schematic diagram is shown in Figure 11. In Figure 11, X direction and  $0^\circ$  overlap, Y direction and  $90^\circ$  overlap, O stands for the sensor. The sensor and the sound source are located in the same plane, and the experimental treatment angle is the horizontal angle and pitching angle is not calculated.

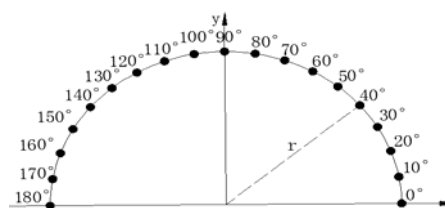


Figure 11. Diagram of the experiment

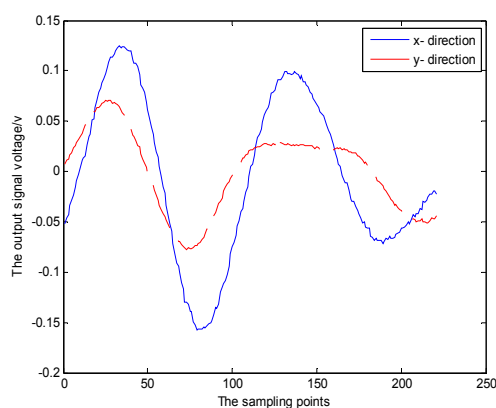
In the Experiment, tapping the ground in the equal diversion point, the sensor will translate acoustic signals collected into electrical signals. The electrical signals are collected by data acquisition card and processed in MATLAB.

Data acquisition card is PXTe-1071 of the NI, and the terminal box is BNC2110. Experimental sampling rate is 10K, and collecting time is 10s. Tap equal diversion point respectively( $r=3.5m$ ), and capture and store the experimental data by the acquisition card and computer. Direction angle can be got by data processing (in Table 1). The results show that the needs of the project will be met within 5 degrees of the mean error of the direction angle.

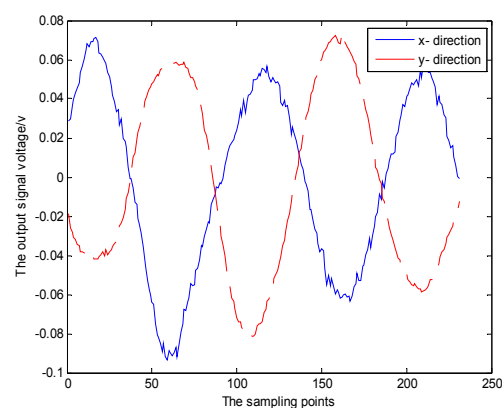
Now we use the examples of  $40^\circ$  and  $140^\circ$  to explain the problem of the port/starboard blur. Tap  $40^\circ$  and  $140^\circ$  equal diversion point once respectively. Signals collected by sensor are shown in Figure 12. Figure 12 (a) shows that  $V_x$  and  $V_y$ , the output voltage collected, change synchronously, and the sound source should be in the first quadrant I; Figure 12 (b) shows that  $V_x$  and  $V_y$ , the output voltage collected, change asynchronously, and the sound source should be in the first quadrant II. Sound source measured are the same with the real station of the sound source, which further proves the correctness of these programs and theories.

Table 1. Result of determination of MEMS acoustic vector sensor

Real angle(°)	Direction angle(°)	error(°)
0	3.4236	3.4236
10	12.3271	2.3271
20	27.7468	7.7468
30	36.9309	6.9309
40	42.6213	2.6213
50	48.9025	-1.0975
60	56.6354	3.3646
70	73.2508	3.2508
80	84.2464	4.2464
90	85.3726	-4.6274
100	99.4331	-0.5669
110	105.8263	-4.1737
120	123.6328	3.6328
130	134.4365	4.4365
140	136.5586	-3.4414
150	156.4202	6.4202
160	158.0138	-1.9862
170	166.2341	-3.7659
180	178.1342	-1.8658



(a) Signal when beating  $40^\circ$



(b) Signal when beating  $140^\circ$

Figure 12. Testing signal

## 5. Conclusion

A MEMS bionic acoustic vector sensor with high sensitivity, good performance in low frequency and lower power has been used in the ground marking. As to the problem of the port/starboard blur of this vector sensor in ground marking, a new scheme has been put forward. By analyzing the theory and mathematical model of the vector sensor structure, it concludes that if  $V_x$  and  $V_y$  change synchronously, the sound source should be in the first quadrant I; if  $V_x$  and  $V_y$  change asynchronously, the sound source should be in the second quadrant II. The results show that the needs of the project will be met within 5 degrees of the mean error of the direction angle. And the correctness of the proposed new program has been further validated.

## References

- [1] Guo Min-zhi, Yang Jia-Yu. Status and development trend of contemporary transportation technology for oil. *China Petroleum and Chemical Industry*. 2004; (7): 16~20.
- [2] Cui Yao-Yao. Study on the Key Technologies in the Racking and Location System of Pipeline Spection Gauge Based on Acoustic Sensor Arrays. PhD Thesis. Tianjin : Tianjin University; 2011.
- [3] Wu Xiao. Research on Above Ground Marking and Tracking of Oil and Gas Pipeline Internal Inspection Instrument Based on Geophone Array. PhD Thesis. Tianjin : Tianjin University; 2011.
- [4] WU Xiao, JIN Shi-jiu, LI Yi-bo. Above-ground marker system of pipeline internal inspection instrument based on geophone array. *Nanotechnology and Precision Engineering*. 2010; 8(6):554.
- [5] GE Xiao-yang, ZHANG Guo-jun, DU Chun-hui. A new MEMS bionic acoustic vector sensor used in above-ground marker of pipeline. *Piezoelectrics & Acoustooptics*. 2012; 34(6):882-885.
- [6] Chen Shang, Xue Chen-yang, Zhang Wen-dong, Fabrication and testing of a silicon-based piezoresistive two-axis accelerometer. *Nanotechnology and Precision Engineering*. 2008; 6(4): 272-277.
- [7] Chen Shang. Research of a Bionic Vector Hydrophone Based on Silicon. PhD Thesis. Taiyuan: North university of China; 2008.
- [8] Xu Jiao, Zhang Guo-jun, Shi Gui-xiong. Advancements in encapsulation of hair vector hydrophone. *Chinese Journal of Sensors and Actuators*. 2011; 24(4): 519-520.
- [9] Liu Lin-xian, Zhang Guo-jun, Xu Jiao. Design and test for a double T-shape MEMS bionic vector hydrophone. *Journal of Vibration and Shock*. 2013; 32(2): 130-131.
- [10] Xu Jiao, Li Jun, Zhang Guo-jun. Design of a novel vector hydrophone based on MEMS. *Piezoelectrics & Acoustooptics*. 2012; 34(1): 90-91.